Available online at www.sciencedirect.com

ScienceDirect

Procedia Structural Integrity 28 (2020) 67–73

Structural Integrity Procedia

www.elsevier.com/locate/procedia

1st Virtual European Conference on Fracture

Graphene oxide does not seem to improve the fracture properties of injection molded PA6

S. Cicero[a,*], J.L. Parra[a], B. Arroyo[a], I.Procopio[a]

[a]*LADICIM - University of Cantabria, E.T.S. de Ingeneros de Caminos, Canales y Puertos, Avda. Los Castros 44, 39005, Santander, Spain*

Abstract

Scientific literature presents a number of examples in which the mechanical properties of materials are significantly improved by adding small amounts of nano-particles. In many cases, the addition of such nano-particles is performed on polymer-matrix composites, with reported improvements in mechanical, optical, thermal or electrical properties. Therefore, the potential of this technology is huge and a great deal of research work is being performed with the aim of generating new advanced engineering materials. However, this paper presents the other side of the coin. The authors have introduced small amounts of Graphene Oxide (up to 1%) in PA6 with the aim of studying their effect on the fracture properties of the resulting composites. For the particular conditions analyzed here, no improvements in the fracture behavior (in both cracked and notched conditions) have been observed (a similar conclusion may be obtained for the tensile behavior). Other types of material properties were not covered in the analysis. Sharing this kind of (negative) results may save other researchers time and budget, and it is a much more common practice in other fields of science.

Keywords: Graphene oxide; PA6; fracture behavior; crack; notch.

1. Introduction

Nano-reinforced composites are a subject of extensive research nowadays. A literature review reveals numerous research papers analyzing how the addition of nano-particles may improve mechanical, optical, thermal or electrical

* Corresponding author. Tel.: +34-942-200-017
E-mail address: ciceros@unican.es

10.1016/j.prostr.2020.10.009

properties, among others. The matrix of the composites can be ceramics (ceramic-matrix nanocomposites), metals (metal-matrix nanocomposites) or polymers (polymer-matrix nanocomposites). Focusing on polymer-matrix composites, typical matrices are epoxy resins (e.g., Hsieh et al. (2010)), PMMA (Cooper et al. (2002)), polyester (e.g., Singh et al. (2002)) or polyamide (e.g., Wan et al. (2013)), among others, whereas examples of nano-reinforcements may be carbon nanotubes, silica nano-particles, nano-clay or graphene oxide (GO) (Zhao et al. (2019), Zhao et al. (2020)). A general observation is that the different papers normally present an enhancement of the material properties being analyzed in each case.

The authors have a certain experience in the fracture analysis of injection molded short glass fibre reinforced polyamide 6 (SGFR-PA6) (e.g., Ibáñez-Gutiérrez et al. (2016), Ibáñez-Gutiérrez and Cicero (2017)) and are currently analyzing the effect of nano-reinforcements on the fracture behavior and the notch effect of engineering polymers. In this context, an experimental program was defined to analyze the fracture behavior and the notch effect on PA6 reinforced with GO (PA6-GO). The references in the literature about this particular combination of mechanical property (fracture behavior), matrix and nano-reinforcement are scarce (e.g., see Zang et al. (2015), Zhao et al. (2019), Zhao et al. (2020)) and do not simply combine the matrix and the reinforcement. Instead, PA-GO powders were subsequently introduced into an epoxy matrix (e.g., Zhao et al. (2019)), or combined with another type of reinforcements such as carbon fiber (e.g., Zhao et al. (2020)). However, Xu and Gao (2010) reported a significant improvement in tensile properties when adding GO (which is reduced to graphene during the polycondensation) into PA6 matrix. Additionally, Liu et al (2015) observed enhanced tensile strength and lower ductility in PA-GO. Given that fracture is a compromise between strength and ductility (Ritchie (2011)), the results obtained by Liu et al. indirectly would question the potential improvement in PA fracture behavior when adding GO.

With all this, the intention of this work is to analyze how the addition of GO affects the fracture behavior at both cracked and notched conditions of PA6-GO nanocomposites obtained by injection molding of PA6 and PA6-GO pellets. Section 2 gathers a description of the materials used and the methodology followed in the research, Section 3 provides the results and the corresponding discussion, and Section 4 summarizes the main conclusions.

2. Materials and methods

The nanocomposite material studied here is composed of PA6 and GO. The PA6 is commercial Ultramid® B3K, an easy flowing stabilized polyamide for fast processing whose typical applications include technical parts with wall thicknesses greater than 2 mm. PA6 is one of the most widely used commercial grades of aliphatic polyamide thanks to its combination of good processability, high mechanical properties, and chemical resistance. In this case, the material was provided in pellets. Its density is 1.13 g/cm3, with nominal elastic modulus, tensile stress and elongation at failure of 3000 MPa, 80 MPa and 20%, respectively. The GO was provided dispersed in Ultramid® B3K pellets with a GO concentration of 1 wt.% (PA-GO1wt%). The lateral size of the GO was 40 µm, the thickness ranging between 1 and 2 nm, the oxygen content being 30%, the BET surface area being 400 m2/g, and the average number of layers ranging between 1 and 2.

Pure PA6 pellets and PA6 pellets containing 1 wt.% of GO were conveniently combined to obtain four nanocomposites with 0 wt.%, 0.25wt.%, 0.50% and 1% of GO (PA/PA-GO1wt% ratios of 1/0, 3/1, 2/2 and 0/1), respectively. The resulting mixtures of pellets were used to fabricate tensile specimens with an Arburg Allrounder 221 K injection-molding machine (Arburg, Lossburg, Germany) in previously fabricated molds, the geometry being shown in Figure 1a. A total amount of 96 specimens were fabricated, 16 of which were initially used in the tensile tests of the four resulting nanocomposites (four tests per material). The tensile tests were performed following ASTM D638 (2010), at room temperature (20 ºC), under displacement control, and using a Servosis ME-405/1 universal test machine (Servosis, Madrid, Spain).

Fracture specimens were obtained from the central part of the remaining 80 tensile specimens, the geometry being shown in Figure 1b. The defects were performed perpendicularly to the longitudinal direction of the original specimens. The notches were obtained by machining, except for those having a 0 mm notch radius (crack-like defects), which were generated by sawing a razor blade. Fracture tests were conducted at room temperature using the same universal test machine, and were performed following ASTM D6068 (2018). Values of K_{mat} (fracture toughness) were obtained for the cracked specimens, whereas for notched specimens K^N_{mat} (apparent fracture toughness) were determined. The latter are the result of applying the formulation of the standard, initially defined for specimens containing crack-like defects, to fracture specimens containing notches.

Once the fracture results (in terms of fracture toughness and apparent fracture toughness) were obtained, the notch effect was analyzed by using the Theory of Critical Distances. This is essentially a group of methodologies, all of them using a characteristic material length parameter (the critical distance, L) when performing fracture assessments (e.g., Taylor (2007), Cicero et al. (2012), Madrazo et al. (2012)). The origins of the TCD date back to the middle of the twentieth century, with the works of Neuber (1958) and Peterson (1959), but in the last two decades this theory has been systematically applied to and validated in different types of materials, processes and material behaviors.

The expression in fracture analysis for the critical distance, L, follows equation (1):

$$L = \frac{1}{\pi}\left(\frac{K_{mat}}{\sigma_0}\right)^2 \quad (1)$$

where K_{mat} is the fracture toughness of the material and σ_0 is the inherent stress, which is usually greater than the elastic limit of the material but requires calibration.

The two best-known methodologies of TCD are the Point Method (PM) and the Line Method (LM). The latter is the one employed in this work to fit the experimental results, and establishes that failure occurs when the average stress from the defect tip along a length equal to 2L reaches the value of σ_0:

$$\frac{1}{2L}\int_0^{2L} \sigma(r)dr = \sigma_0 \quad (2)$$

The LM is able to predict the apparent fracture toughness (K^N_{mat}) for U-shaped notches when combined with the linear-elastic stress distribution in the notch tip proposed by Creager-Paris (1967):

$$\sigma(r) = \frac{K}{\sqrt{\pi}}\frac{2(r+\rho)}{(2r+\rho)^{\frac{3}{2}}} \quad (3)$$

The combination of equations (2) and (3) leads to Equation (4), which allows K^N_{mat} to be predicted as a function of the fracture toughness of the material, K_{mat}, the notch radius, ρ, and the critical distance, L.

$$K^N_{mat} = K_{mat}\sqrt{1+\frac{\rho}{4L}} \quad (4)$$

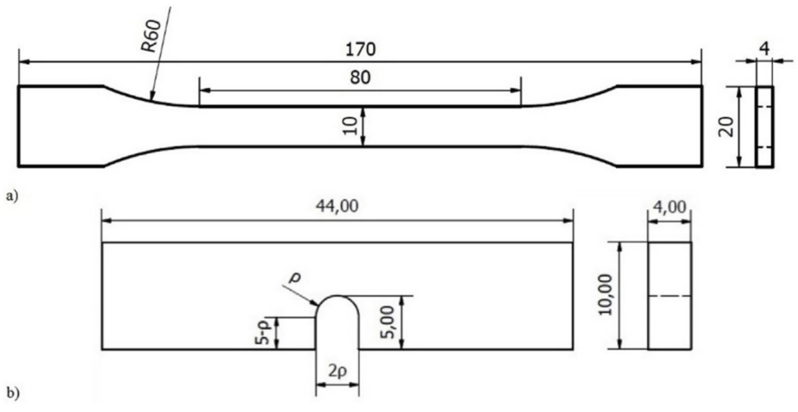

Fig. 1. (a) Tensile specimen (mm); (b) SENB specimens (mm) with notch radius (ρ) varying from 0 to 2 mm.

3. Results and discussion

Figure 2 presents some of the results of the tensile tests. For each GO content, one curve has been included. There were no significant deviations between the different tensile curves of each particular nanocomposite. Table 1 presents the resulting average values. It can be observed that strength parameters do not improve with the addition of GO. If any, the tendency is to slight reductions of such parameters when the GO content increases. Concerning the ductility, there is no clear improvement either, although there might be an increase in the ductility when the GO is added.

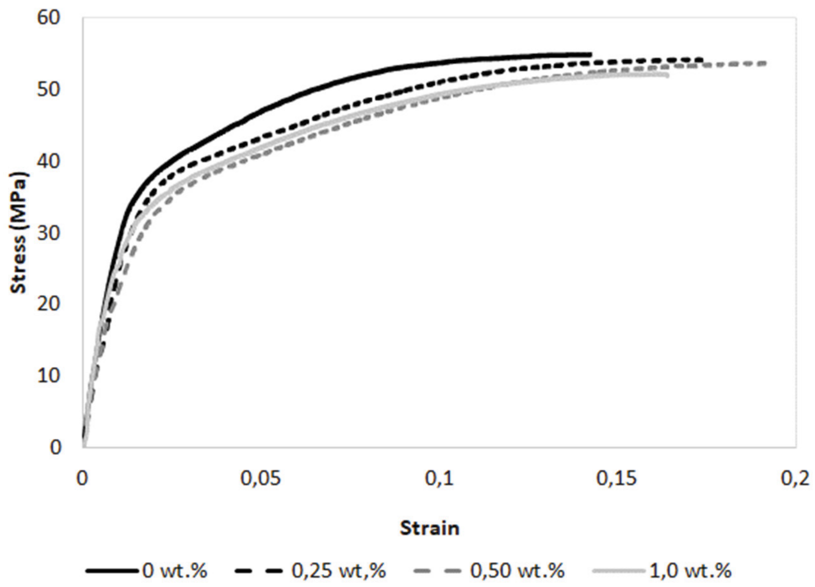

Fig. 2. Examples of tensile curves for the four different contents of GO (wt.%).

Table 1. Tensile properties (average values)

GO content (wt.%)	E (MPa)	$\sigma_{0.2}$ (MPa)	σ_u (MPa)	ε_{max} (%)
0.0	3099	31.63	55.23	14.03
0.25	3127	29.54	54.27	16.08
0.50	3100	31.67	53.50	13.87
1.0	2732	28.21	52.97	16.18

Figure 3 presents some of the load-displacement curves of the fracture tests. Figure 4 presents the evolution of the apparent fracture toughness in the four resulting nanocomposites, showing the results of all the tested specimens. The results have been fitted to equation 4 (Figure 5) by using the least squares methodology and with L being the fitting parameter. It can be observed how the fracture behavior does not improve with the GO content. On the contrary, the highest values of fracture toughness and apparent fracture toughness are generally observed in pure PA6.

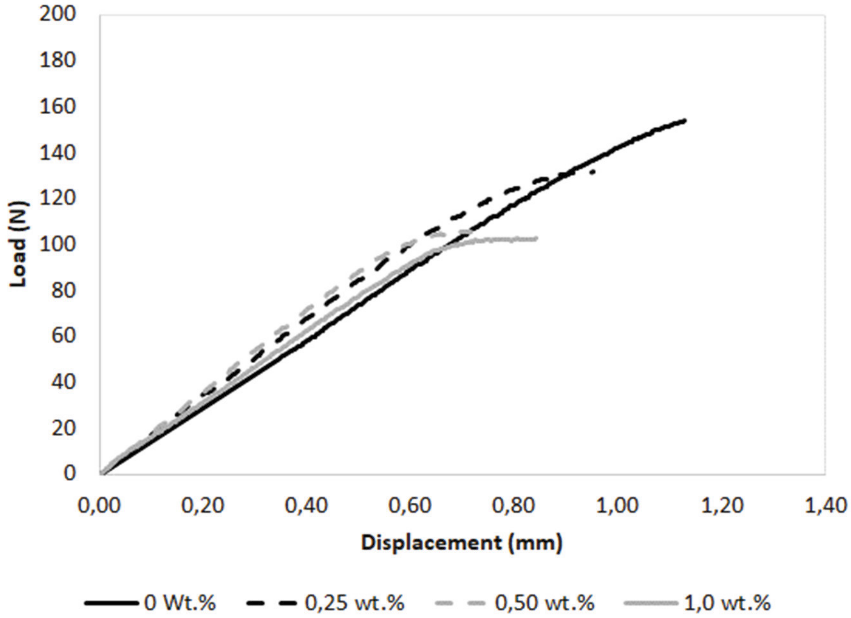

Fig. 3. Examples of load-displacement curves obtained for fracture specimens with different amounts of GO (wt.%). All the represented specimens contain crack-like defects (note that the crack lengths are not exactly the same).

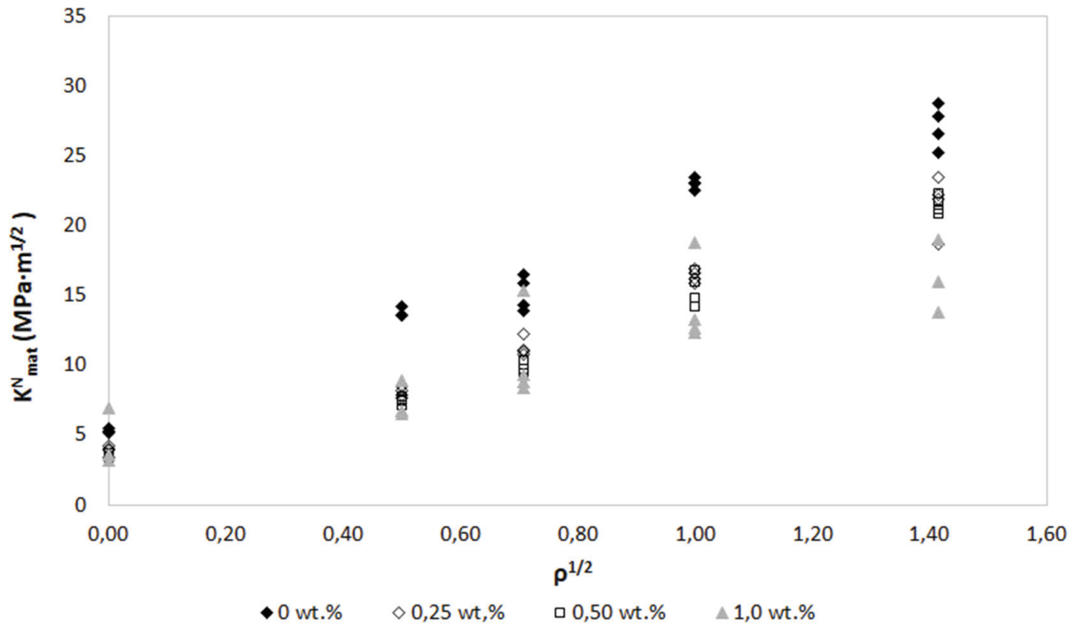

Fig. 4. Evolution of fracture resistance with notch radius for the different contents of GO.

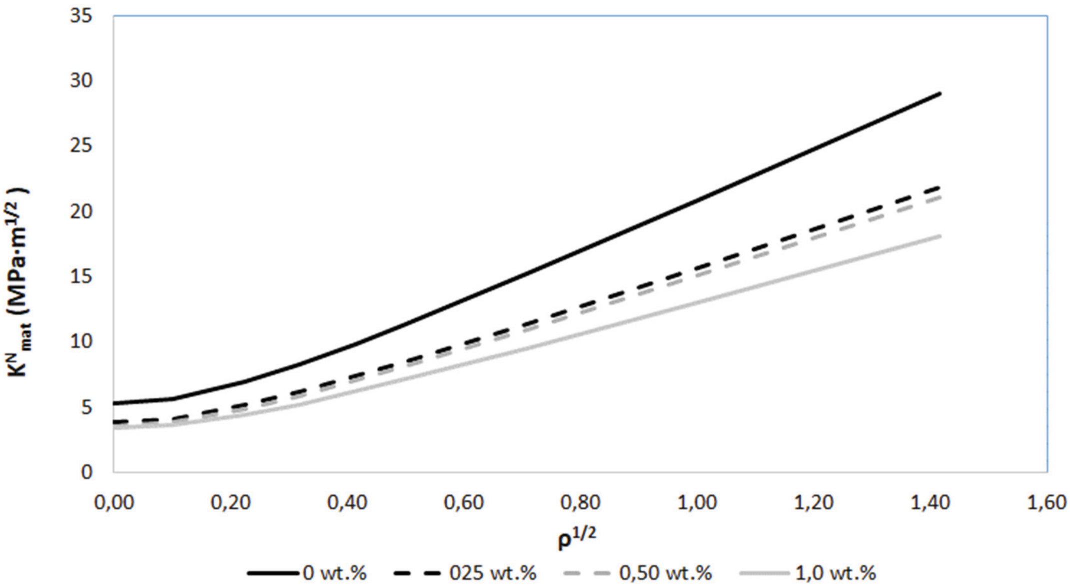

Fig. 5. LM best-fit curves for the different contents of GO.

The notch effect (i.e., the increase in the fracture resistance with the notch radius) is very similar for the four nanocomposites. In fact, L, which measures the sensitivity of the material to the notch effect, is 0.017 mm, 0.016 mm, 0.015 mm, and 0.019 mm for the materials containing 0 wt.%, 0.25 wt.%, 0.50 wt.% and 1.0 wt.% of GO. These modest differences are even less significant if it is considered that L is squared in equation (4).

In order to justify all these observations, further research is being performed related with fracture micromechanisms and the dispersion of GO within the PA6. Preliminary results show very similar fracture micromechanisms in the four analyzed materials, regardless of the GO content. This would justify why GO does not improve the fracture behavior. Moreover, the lack of positive effect could be hypothetically attributed to a bad dispersion of the GO within the matrix. However, this possibility loses reliability when it is considered that PA-GO1wt% dispersion is performed and guaranteed in origin by the material supplier, and the corresponding fracture behavior is not better than that observed in pure PA6.

4. Conclusions

Driven by the reported potential of nano-reinforcements for the improvement of the mechanical properties of polymer-matrix nanocomposites, the authors have analyzed how graphene oxide (GO) affects the fracture behavior of PA6. The analysis has been performed on injection molded PA6 containing different contents of GO (0 wt.%, 0.25 wt.%, 0.50 wt.%, and 1.0 wt.%) and notches with variable radii (0 mm, 0.25 mm, 0.50 mm, 1.0 mm and 2.0 mm). The main conclusions are the following:

- GO generates slight reductions in the strength (tensile) properties of PA6, as well as a slight increase in ductility.
- GO does not improve the fracture resistance of PA6 for the specific conditions analyzed in this work. On the contrary, the highest fracture resistance has been observed in pure PA6.
- GO does not significantly affect the notch effect observed in pure PA6.

Other material properties have not been analyzed in this research.

Acknowledgements

The authors of this work would like to express their gratitude to the Spanish Ministry of Science and Innovation for the financial support of the project PGC2018-095400-B-I00 "Comportamiento en fractura de materiales compuestos nano-reforzados con defectos tipo entalla", on the results of which this paper is based.

References

Ajayan, P.M., Schadler, L.S., Giannaris, C., Rubio, A., 2000. Single-walled carbon nanotube-polymer composites: Strength and weakness. Advanced Materials 12, 750-753.

ASTM D6068-10(2018), 2018. Standard Test Method for Determining J-R Curves of Plastic Materials. ASTM International, West Conshohocken, PA, USA.

ASTM D638-14, 2014. Standard Test Method for Tensile Properties of Plastics. ASTM International, West Conshohocken, PA, USA.

Cicero, S., Madrazo, V., Carrascal, I.A., 2012. Analysis of notch effect in PMMA by using the theory of critical distances. Engineering Fracture Mechanics 86, 56-72.

Cooper, C.A., Ravich, D., Lips, D., Mayer, J, Wagner, H.D., 2002. Distribution and alignment of carbon nanotubes and nanofibrils in a polymer matrix. Composites Science and Technology 62, 1105-1112.

Creager, M., Paris, P., 1967. Elastic field equations for blunt cracks with reference to stress corrosion cracking. International Journal of Fracture Mechanics 3, 247–252.

Hsieh, T.H., Kinloch, A.J., Masania, K., Sohn Lee, J., Taylor, A.C., Sprenger, S., 2010. The toughness of epoxy polymers and fibre composites modified with rubber microparticles and silica nanoparticles. Journal of Materials Science 45, 1193-1210.

Ibáñez-Gutiérrez, F.T., Cicero, S., Carrascal, I.A., Procopio, I., 2016. Effect of fibre content and notch radius in the fracture behavior of short glass fibre reinforced polyamide 6: An approach from the Theory of Critical Distances, Composites Part B: Engineering 94, Pages 299-311

Ibáñez-Gutiérrez, F.T., Cicero, S., 2017. Fracture assessment of notched short glass fibre reinforced polyamide 6: An approach from failure assessment diagrams and the theory of critical distances. Composites Part B: Engineering 111, 124-133.

Liu, X., Guan, Y., Shao, X., Zhao, L., He, H., 2015. Preparation and properties of graphene oxide /nylon nanocomposites. Polymeric Materials Science and Engineering 31, 165-169 and 174.

Madrazo, V., Cicero, S., Carrascal, I.A., 2012. On the point method and the line method notch effect predictions in Al7075-T651. Engineering Fracture Mechanics 79, 363-379.

Neuber, H., 1958. Theory of notch stresses: principles for exact calculation of strength with reference to structural form and material, Springer. Verlag, Berlin, Germany.

Peterson, R.E., 1959. Notch sensitivity, in "*Metal Fatigue".* McGraw Hill, New York, USA, pp. 293–306.

Ritchie, R.O., 2011. The conflicts between strength and toughness. Nature Materials 10, 817-822.

Singh, R.P., Zhang, M., Chan, D., 2002. Toughening of a brittle thermosetting polymer: Effects of reinforcement particle size and volume fraction. Journal of Materials Science 37, 781-788.

Taylor, D., 2007. The theory of critical distances: a new perspective in fracture mechanics. Elsevier, London, UK.

Wan, T., Liao, S., Wang, K., Yan, P., Clifford, M., 2013. Multi-scale hybrid polyamide 6 composites reinforced with nano-scale clay and micro-scale short glass fibre. Composites Part A: Applied Science and Manufacturing 50, 31-38.

Xu, Z., Gao, C.E., 2010. In situ polymerization approach to graphene-reinforced nylon-6 composites. Macromolecules 43, 6716-6723

Zang, C.G., Zhu, X.D., Jiao, Q.J., 2015. Enhanced mechanical and electrical properties of nylon-6 composite by using carbon fiber/graphene multiscale structure as additive. Journal of Applied Polymer Science 132, 41968.

Zhao, X., Li, Y., Chen, W., Li, S., Zhao, Y., Du, S., 2019. Improved fracture toughness of epoxy resin reinforced with polyamide 6/graphene oxide nanocomposites prepared via in situ polymerization. Composites Science and Technology 171, 180-189.

Zhao, X., Chen, W., Han, X., Zhao, Y., Du, S., 2020. Enhancement of interlaminar fracture toughness in textile-reinforced epoxy composites with polyamide 6/graphene oxide interlaminar toughening tackifier. Composites Science and Technology 191, 108094.